

# BL33XU TOYOTA

## 1. Introduction

The BL33XU Toyota beamline was built in FY2009 and is operated by Toyota Central R&D Labs., Inc. [1]. The original purpose of this beamline was to perform quick-scanning X-ray absorption spectroscopy (QXAFS) for operando analysis and three-dimensional X-ray diffraction (3DXRD). These techniques were unavailable at SPring-8 before 2009 and needed for industrial applications. In addition to these, the following techniques have been adopted: X-ray diffraction (XRD), X-ray computed tomography (CT)/laminography, and small-angle X-ray scattering (SAXS), as shown in Fig. 1. In this report, we describe the current status of this beamline and recent technical progress.

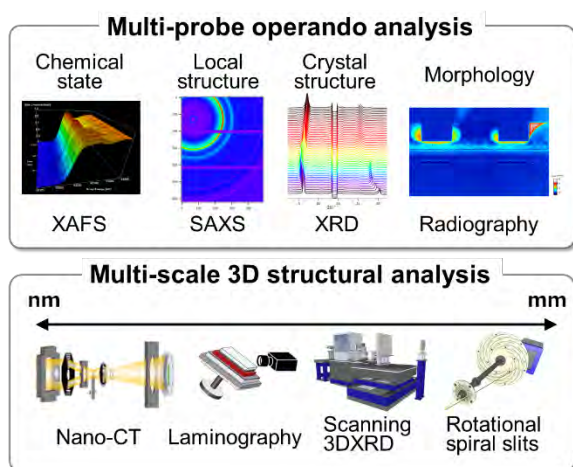


Fig. 1. Measurement techniques at BL33XU.

## 2. BL33XU beamline

### 2-1. Beamline layout

The medium-length beamline of BL33XU has the optics hutch in the storage ring building of SPring-8. The experimental facility building is located outside the storage ring building. It has three experimental hutches, a chemical laboratory, and an

office room.

The layout of the optical components of BL33XU, where two different types of monochromators are installed, is shown in Fig. 2. Optics 1 is mainly used for QXAFS. It is composed of horizontal deflection mirrors (M1 and M2) in the optics hutch, compact monochromators (C-Mono) with channel-cut crystals, and vertical deflection mirrors (M3 and M4) in the experimental hutch 1. Optics 2 is used for 3DXRD and other techniques. It consists of a SPring-8 standard double-crystal monochromator, vertical deflection mirrors (M4 and M5), and Kirkpatrick–Baez focusing mirrors (KBM) that yield a 1- $\mu\text{m}$ -square microbeam at 50 keV in the experimental hutch 3.

### 2-2. Analysis techniques

#### (1) QXAFS

A tapered undulator combined with the servo-motor-driven channel-cut monochromator realizes rapid data acquisition of XAFS with a temporal resolution of 10 ms [2]. The energy range from 4.0 to 45 keV is accomplished by the two monochromators with Si(111) and Si(220) crystals. This QXAFS system has enabled the development of various *in situ* measurement techniques such as

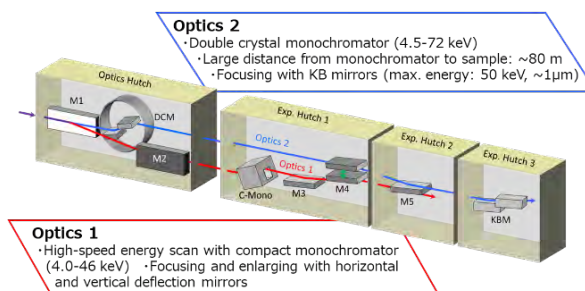


Fig. 2. Optical components of BL33XU.

simultaneous XAFS and XRD measurements of positive and negative electrodes of lithium-ion batteries during charging and discharging [3].

## (2) SAXS

For SAXS at BL33XU, the camera distance can be selected from tens of centimeters to 4.5 meters. A two-dimensional detector, PILATUS 300K (Dectris), is available for the developed *in situ* measurement system. An example task is an *in situ* measurement to analyze the structural evolution of resins during the injection molding process [4].

## (3) XRD

To analyze the reliability of mechanical and electronic components, it is important to measure the internal stresses and strains nondestructively. The measurement based on XRD was realized by using a multi-axial goniometer equipped with a newly developed rotating and revolving spiral slits system. The rotating shield disks with the slits enable the detection of diffraction only from a small gage volume of interest inside a component with a two-dimensional detector, PILATUS. This system realizes the depth-resolved distribution measurement of strains in an actual mechanical component [5].

## (4) Scanning 3DXRD

To measure the three-dimensional distribution of stresses inside the grains of a bulk sample, i.e., type III stresses, the scanning three-dimensional X-ray diffraction (3DXRD) microscopy methodology was developed [6]. This nondestructive technique was validated in 2013, and the three-dimensional distribution of stresses inside the grains of bulk polycrystalline steel under tensile deformation was measured in 2019 [7]. The results revealed that the microscopic intragranular stresses considerably deviate from the macroscopic average stresses

measured by conventional methods. Combined with other nondestructive measurement techniques such as XRD and laminography, 3DXRD is expected to facilitate the development of multiscale material modeling that expresses deformation, fracture, and life of components.

## (5) X-ray CT and laminography

To meet the growing need for the high-resolution, nondestructive observation of internal behavior in mechanical and electronic components, X-ray CT and laminography techniques were introduced. The resolutions of the two imaging techniques are better than 1  $\mu\text{m}$  even under *in situ* measurement where sample materials and components are exposed to actual working conditions. A newly adopted CT system with a Fresnel zone plate (FZP) has achieved a resolution of  $\sim 100$  nm.

## 3. Recent technological progress: Nondestructive crystal orientation analysis of solder joints on electronic substrates by scanning 3DXRD

In the efforts towards a carbon-neutral society, with the progression of vehicle electrification, ensuring the high reliability of in-vehicle electronic equipment has become increasingly important. Electronic boards, the central components of electronic equipment, are typically constructed by densely mounting IC chips and printed circuit boards (PCBs) using ball grid array (BGA) solder. Under extreme operating conditions, degradation could occur in solder joints. Therefore, it is important to measure changes in crystalline orientation that correlate with solder degradation.

To this end, scanning 3DXRD, a technique established at BL33XU, was applied to analyze solder crystal orientation [8].

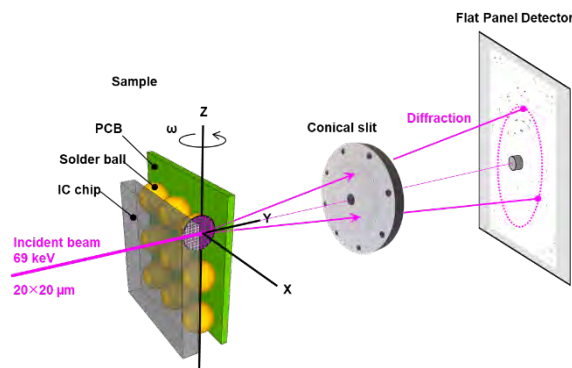


Fig. 3. Schematic layout of full-size electronic substrate measurement by scanning 3DXRD.

The layout of the experimental setup is shown in Fig. 3. Incident X-rays, monochromatized to 69 keV by a Si311 monochromator and shaped to a 20  $\mu\text{m}$  square by a four-quadrant slit, were used. The measurement sample was a 120  $\times$  160 mm full-size electronic board, on which X-rays were aimed at solder balls of about 0.5 mm diameter under the IC chips mounted on the board. A flat panel detector (FPD) with a pixel resolution of 75  $\mu\text{m}/\text{pixel}$  was used. A conical slit was placed between the measurement sample and the FPD to selectively guide only the diffraction from the solder balls ( $\beta$ -Sn) to the FPD. The sample was scanned in the YZ 2D plane, and a crystallographic orientation map of one cross section through the center of the solder ball was drawn by indexing the diffraction spot data set at each measurement point.

Figure 4 shows the crystallographic orientation map of the solder balls in the electronic board's initial state. Previous studies using electron backscatter diffraction (EBSD) have demonstrated that solder balls on electronic substrates generally

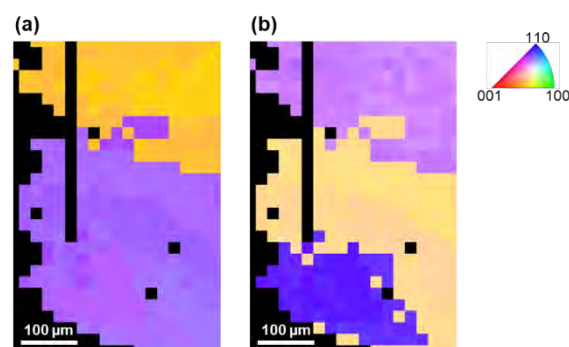


Fig. 4. Crystal orientation maps in (a) ND (X) and (b) TD (Z) directions. The black areas indicate measurement points that were not indexed.

comprise a few particles. The solder balls measured in this experiment were composed of three coarse particles. Although the positional resolution is lower than that of EBSD, scanning 3DXRD has the significant advantage of not requiring the preparation of cross-sectional samples for the measurement, and the orientation information can be obtained nondestructively. It is known that solder undergoes grain refinement and changes in crystal orientation with increased intraparticle strain during cold/heat cycle tests that simulate the actual operating environment. This technology, which enables the nondestructive and traceable measurement of these changes, will significantly contribute to the reliable design of electronic substrates.

KISHIDA Yoshihiro

Toyota Central R&D Labs., Inc.

#### References:

- [1] Nonaka, T. et al. (2016). *AIP Conf. Proc.* **1741**, 030043.
- [2] Nonaka, T. et al. (2012). *Rev. Sci. Instrum.* **83**, 083112.

- [3] Makimura, Y. et al. (2016). *J. Electrochem. Soc.* **163**(7), A1450–A1456.
- [4] Harada, M. et al. (2015). *SPring-8 User Experiment Report* 2015A7003, 2015B7003.
- [5] Setoyama, D. et al. (2015). *Proc. MECASENSE 2015*, 4.
- [6] Hayashi, Y. et al. (2017). *SPring-8 User Experiment Report*, 2017A7002, 2017B7002.
- [7] Hayashi, Y. et al. (2019). *Science* **366**, 1492–1496.
- [8] Kishida, Y. et al. (2023). *SPring-8 User Experiment Report*, 2023A7044.